J Therm Anal Calorim
DOI 10.1007/s10973-014-3638-1

Structure investigation of mesalazine drug using thermal analyses, mass spectrometry, DFT calculations, and NBO analysis

Mostafa Y. Nassar · M. F. El-Shahat · S. M. Khalile · M. El-Desawy · Eman A. Mohamed

Received: 18 August 2013 / Accepted: 4 January 2014

Abstract Mesalazine (MZ) drug has been used for several decades as a primary treatment for inflammatory bowel diseases. The drug was investigated using thermal analysis (TA) measurements and electron impact mass spectral fragmentation at 70 and 15 eV of electron energy. The optimum molecular geometry and the total energy of the neutral and the positively charged MZ molecules were calculated by density functional theory method with 6-311++G(d,p) basis sets. Stability of the molecules arising from hyperconjugative interactions, charge delocalization, and the natural atomic charges has been analyzed using natural bond orbital analysis. In electron ionization mass spectrometry, the primary rupture is due to successive loss of H_2O (OH from carboxyl and H from phenolic OH of the ring) and CO of the acetyl group. Thermogravimetric results have revealed two stages of mass loss at 75.3 and 25.3 % in ranges 225–350 and 350–650 °C, respectively. The first one may be due to successive losses of different groups or molecules with fast rate of decomposition. A comparison between MS and TA helped in selection the proper pathway representing the fragmentation mechanism of this drug.

Keywords Mesalazine · Mass spectroscopy · Thermal analysis · DFT calculations · NBO analysis · Structure reactivity relationship

M. Y. Nassar (✉)
Chemistry Department, Faculty of Science, Benha University, Benha 13518, Egypt
e-mail: m_y_nassar@yahoo.com; m_y_nassar@fsc.bu.edu.eg

M. F. El-Shahat (✉)
Chemistry Department, Faculty of Science, Ain Shams University, Abbasia, Cairo 11566, Egypt
e-mail: elshahatmf@hotmail.com

S. M. Khalile
National Organization for Drug Control and Research (NODCAR), Giza, Egypt

M. El-Desawy
Nuclear Physics Department, Nuclear Research Centre, AEA, 13759 Cairo, Egypt

E. A. Mohamed
National Cancer Institute, (NCI), Cairo, Egypt

Introduction

Mesalazine (MZ, $C_7H_7NO_3$, MW = 153) drug known as mesalamine or 5-aminosalicylic acid (5-ASA) is one of the most commonly used drugs for the treatment of active inflammatory bowel diseases (IBD) and for maintenance of remission [1–3]. Mass spectrometry (MS) has become a power tool for drug metabolism studies [4]. The technique is important because it provides a large amount of structural information with little expenditure of sample [5–8]. Despite the importance of this drug in medicine, to the best of our knowledge, the fragmentation mechanisms of the title compound along with thermal studies have not been reported. Thermal analytical techniques can provide important information regarding storage and stability of pharmaceuticals. Thermal analytical methods have thus become important tools for the development of modern medicines [9–13]. Thermogravimetric TG/DTG analysis was used to provide quantitative information on mass losses due to decomposition and/or evaporation of low molecular materials as a function of time and temperature [14–16]. In conjunction with mass spectrometric analysis [17–19], the nature of the released volatilize may be deduced, thus greatly facilitating the interpretation of

Published online: 02 February 2014

thermal degradation processes. In literatures, to the best of our knowledge, the thermal stability of the drug with temperature change, either in vitro or in vivo systems, has not been studied except the coordinated drug with some metal ions [8].

On the other hand, computational quantum chemistry can provide additional information about the atoms and bonds, which can be used successfully in an interpretation of experimental results such as thermal analysis (TA) and MS experimental results [20]. These theoretical data can particularly be valuable for MS scientists. In such, a number of articles [21–24] dealt with a combined experimental work (TA and MS) and a semi-empirical calculation. Although this kind of combination gives good information about both atoms and bonds, however, the used semi-empirical calculations in the reported studies are not accurate enough compared with the density functional theory (DFT) calculations which have been applied in this work.

The aim of the present work is to carry out experimental and theoretical investigation on MZ using electron impact mass spectral (EI-MS) fragmentation at 70 and 15 eV of electron energy, and TA measurements. DFT calculation and natural bonding orbital (NBO) analysis were performed on the neutral MZ molecule and its positively charged molecular ion to investigate different geometrical parameters (such as bond order, natural atomic charge, and bond length) and donor–acceptor interactions which in turn were used to rationalize the correct pathway of fragmentation for each technique.

Experimental

Materials

Mesalazine (MZ, M.wt. = 153 g mol^{-1}), as an authentic sample, was kindly supplied by Egyptian Drug Control Authority (EDCA), Cairo (Egypt).

Mass spectrometry

Electron ionization mass spectra of MZ were obtained using Thermo Finnigan TRACE DSQ quadruple mass spectrometer with electron multiplier detector equipped with GC–MS data system. The direct probe (DP) for solid material was used in this study. The sample was put into a glass sample micro vial, by a needle ($\approx$1 μg max), the vial installed on the tip of the DP containing heating cable and inserted into the evacuated ion source. The sample was ionized by electron beam emitted from the filament, the generated ions being effectively introduced into the analyzer by the focusing and extractor lenses system. The MS was continuously scanned and the obtained spectra were stored. Electron ionization mass spectra were obtained at ionizing energy value of 70 and 15 eV, ionization current of 60 μA and vacuum is better that 10^{-6} torr.

Thermal analyses (TA)

The thermogravimetric (TG/DTG) analysis was carried out in dynamic nitrogen atmosphere (20 mL min^{-1}) with a heating rate of 10 °C min^{-1} using Shimadzu TGA-50H and DTA-50H thermal analyzers. In the present investigation, heating rates were suitably controlled at 10 °C min^{-1} under nitrogen atmosphere and the mass loss is measured from the ambient temperature up to $\cong$700 °C.

Computational method

The optimized molecular structure of the title compound and corresponding energy were calculated by using GAUSSIAN 09 program package [25] using DFT with Becke3–Lee–Yang–Parr (B3LYP) [26, 27] combined with 6-311++G(d,p) basis set without any constraint on the geometry. The NBO calculation was performed using NBO 3.1 program [28] and was carried out in the Gaussian 09 W package at the DFT/B3LYP level. The hyperconjugative interaction energy was deducted from the second order perturbation approach [29–31]. Gaussview program [32] has been considered to get visual the optimized structures. It is worthy to mention that at the optimized geometry for the title molecule (the neutral and the positively charged one) no imaginary frequency modes were obtained.

Results and discussion

It is of great interest to study the chemistry and reactivity of MZ drug because of its importance in medicine. It is difficult to establish the exact major fragmentation pathway in EI using conventional MS. With combining the above two techniques and the data obtained from both the DFT calculation and NBO analysis, it is possible to understand the following topics:

1. Stability of the drug under thermal degradation in solid state and mass spectral fragmentation in gas phase.
2. Prediction of the primary site of fragmentation and subsequent bond cleavage.
3. The correct pathway in both techniques.

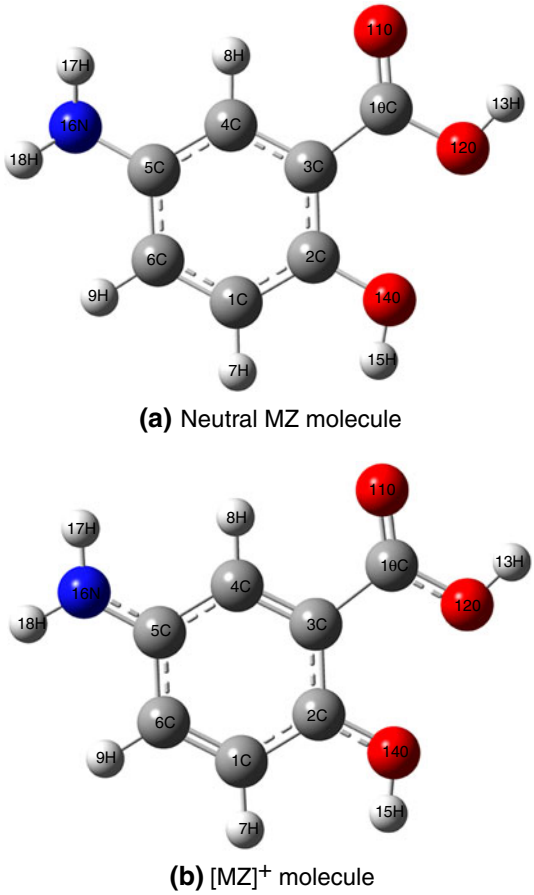

Fig. 1 Optimized geometrical structure of mesalazine along with numbering of atoms: **a** Neutral MZ and **b** positively charged MZ

Molecular geometry and NBO analysis

The DFT calculation and NBO analysis gave valuable information about the structure and reactivity of the molecules, which actually could be used to support the experimental evidence. The much important parameters calculated using DFT calculation and NBO analysis are bond length, Mulliken atomic charge distribution, bond order, natural atomic charge distribution, donor–acceptor interactions, and the corresponding total energy. In the present work, the calculations have been carried out on MZ; neutral molecule (related to TA decomposition) and charged molecular ion (related to MS fragmentation), which have been then used for prediction of the weakest bond rupture to follow the fragmentation pathways in both techniques.

The molecular structures along with numbering of atoms of the neutral and positively charged MZ molecule are shown in Fig. 1. The global minimum energy obtained by the DFT structure optimization based on B3LYP with 6-311++G(d,p) basis set for neutral and positively charged MZ molecule is −551.56236266 and −551.29475163 a.u., respectively. Consequently, the neutral MZ molecule is more stable than the positively charged one because it has lower total energy. The most optimized structural parameters (bond length) B3LYP with 6-311++G(d,p) basis set, and the bond order performed for the optimized structures using NBO 3.1 program implemented in the Gaussian 09 package are presented in Table 1.

Table 1 Selected optimized geometrical parameters; bond length and bond order, for neutral and positively charged MZ drug

Bond	Bond length/Å		Bond order	
	Neutral MZ	MZ cation	Neutral MZ	MZ cation
C1–C2	1.3987	1.4258	1.3638	1.2305
C1–C6	1.3866	1.3636	1.4619	1.5989
C2–C3	1.4079	1.432	1.3155	1.2050
C2–O14	1.3647	1.3193	1.0318	1.1743
C3–C4	1.4033	1.3733	1.3720	1.5394
C3–C10	1.4899	1.5154	1.0250	0.9717
C4–C5	1.3921	1.4249	1.3855	1.2045
C5–C6	1.4022	1.4286	1.3333	1.1959
C5–N16	1.4026	1.3393	1.1045	1.3363
C10–O11	1.2131	1.2032	1.7058	1.7546
C10–O12	1.3497	1.3328	1.0552	1.0920

When comparing among the bond length, bond order, and total energy values present in Table 1 for the neutral and positively charged drug, one can conclude the following:

i. Small differences in bond length in MZ system upon ionization, indicating that no appreciable change in the geometries upon ionization.
ii. The lowest bond order (important for prediction of primary site of cleavage) observed at bond C3–C10 for both neutral (1.0250) and positive species (0.9717).
iii. Upon ionization the stability of the molecule decreased by 167.928 kcal mol^{-1}.

Mulliken atomic charge calculation has an important role in the application of quantum chemical calculation to molecular system. The total atomic charges of neutral and charged MZ species obtained by Mulliken using B3LYP/6-311++G(d,p) and NBO methods are listed in Table 2. The two methods predict the same tendencies especially in the case of oxygen and carbon atoms. Significant changes in the electron distribution with given system often take place during the ionization process [33]. Actually, both methods especially the NBO method predict that the greatest change occurred in charge distribution as a result of electron rupture upon ionization occurs at N16 [from −0.59783 to (−0.79436) ≈ 0.20)].

Table 2 The charge distribution calculated by the Mulliken (B3LYP/6-311++G(d,p)) and natural bond orbital (NBO) methods

Atoms	Atomic charges/Mulliken		Natural charges/NBO	
	Neutral MZ	MZ cation	Neutral MZ	MZ cation
C1	−0.027263	0.013209	−0.26171	−0.21793
C2	−1.050374	−1.095095	0.32716	0.43402
C3	0.678340	0.805435	−0.19836	−0.15109
C4	0.015032	−0.138899	−0.18172	−0.12652
C5	−0.724146	−0.551188	0.13541	0.21730
C6	0.290912	0.346955	−0.20027	−0.16188
H7	0.129298	0.202816	0.20022	0.23673
H8	0.187311	0.236458	0.22889	0.26019
H9	0.158532	0.218092	0.20325	0.23763
C10	0.288005	0.371696	0.79193	0.78726
O11	−0.306565	−0.238587	−0.62023	−0.55945
O12	−0.183781	−0.168186	−0.66297	−0.64678
H13	0.305505	0.341050	0.47954	0.50459
O14	−0.202852	−0.080066	−0.65252	−0.54973
H15	0.267486	0.311316	0.46383	0.49623
N16	−0.306396	−0.227165	−0.79436	−0.59783
H17	0.241154	0.321513	0.37290	0.42017
H18	0.239801	0.330649	0.36901	0.41710

Natural bond orbital (NBO) analysis

The natural bond orbital (NBO) calculation was performed using NBO 3.1 program implemented in the Gaussian 09 package at the DFT/B3LYP/6-311++G(d,p) level in order to understand intra- and inter-molecular bonding and interaction among bonds, which is a measure of the delocalization or hyperconjugation. The hyperconjugative interaction energy was deduced from the second-order perturbation approach [34]. Delocalization of electron density between occupied Lewis-type (bond or lone pair) NBO orbitals and formally unoccupied (antibond or Rydberg) non-Lewis NBO orbitals corresponds to a stabilizing donor–acceptor interaction. In NBO analysis, the larger the $E^{(2)}$, the more intensive is the interaction between electron donors and electron acceptors, i.e., the more donating tendency from electron donors to electron acceptors and the greater the extent of conjugation of the whole system. The possible intensive interactions are given in Tables 3 and 4 for the neutral and positively charged MZ molecules, respectively. Delocalization of electrons of the neutral MZ is higher than that of the positively charger MZ and this results in increase in the stability of the neutral MZ in comparing to the $[MZ]^+$. For example, as shown in Table 3, π(C1–C6) → π*(C2–C3), π(C2–C3) → π*(C4–C5), π(C4–C5) → π*(C1–C6) interactions are seen for MZ to give strong stabilization of 20.22, 20.88, and 21.48 kcal mol^{-1}, respectively. Also, as presented in

Table 3 Significant donor–acceptor interactions of neutral MZ molecule and their second order perturbation energies

Donor NBO_i	Acceptor NBO_j	E'/ kcal mol^{-1}	ΔE/ a.u.	F/ a.u.
BD(2) C1–C6	BD*(2) C2–C3	20.22	0.28	0.071
BD (2) C1–C6	BD*(2) C4–C5	16.76	0.30	0.064
BD (2) C2–C3	BD*(2) C1–C6	18.39	0.28	0.064
BD (2) C2–C3	BD*(2) C4–C5	20.88	0.29	0.070
BD (2) C2–C3	BD*(2) C10–O11	20.97	0.27	0.069
BD (2) C4–C5	BD*(2) C1–C6	21.48	0.28	0.069
BD (2) C4–C5	BD*(2) C2–C3	19.11	0.27	0.066
LP (1) O11	RY*(1) C10	15.63	1.86	0.152
LP (2) O11	BD*(1) C3–C10	17.50	0.69	0.100
LP (2) O11	BD*(1) C10–O12	31.70	0.62	0.126
LP (2) O12	BD*(2) C10–O11	45.14	0.34	0.113
LP (2) O14	BD*(2) C2–C3	28.57	0.34	0.096
LP (1) N 16	BD*(2) C4–C5	23.79	0.33	0.084
BD*(2) C1–C6	BD*(2) C4–C5	263.44	0.01	0.082
BD*(2) C2–C3	BD*(2) C4–C5	243.80	0.01	0.078
BD (1) C3–C4	BD*(1) C2–O14	4.16	1.04	0.059
BD (1) C3–C4	BD*(1) C5–N16	3.89	1.12	0.059

E' means energy of hyperconjugative interactions $[E^{(2)}]$

$\Delta E = E_j - E_i$ is the energy difference between donor (i) and acceptor (j) NBO orbitals; $F = F(i, j)$ is the Fock matrix element between i and j NBO orbitals

Table 4, π(C1–C2) → π*(C3–C4), π(C3–C4) → π*(C5–C6), π(C5–C6) → π*(C1–C2) interactions are seen for $[MZ]^+$ to give a lower stabilization of 9.72, 9.94, and 12.34 kcal mol^{-1}, respectively. However, the strong stabilization denotes the larger delocalization in the neutral MZ compared to that of $[MZ]^+$ molecule. However, the most important interactions of MZ molecule having lone pair LP(2) O11 with that of antibonding BD*(1) C3–C10 and BD*(1) C10–O12 result in the stabilization energy of 17.50 and 31.70 kcal mol^{-1}, respectively. Consequently, it can be concluded that the antibonding BD*(1) C10–O12 has higher electron density than that of BD*(1) C3–C10, and hence the rupture of the C10–O12 bond may be easier compared to C3–C10. The same trend and conclusion can be obtained for the same two bonds in $[MZ]^+$ molecule, since the interaction of LP(2) O11 in this molecule with BD*(1) C3–C10 and BD*(1) C10–O12 has stabilization energy of 10.55 and 15.59 kcal mol^{-1}, respectively.

Mass spectral (MS) fragmentation of MZ drug

Electron ionization mass spectra of MZ drug were measured and investigated at 70 and 15 eV of electron energy.

Table 4 Significant donor–acceptor interactions of positively charged MZ molecule and their second order perturbation energies

Donor NBO_i	Acceptor NBO_j	E'/ kcal mol^{-1}	ΔE/ a.u.	F/ a.u.
BD (2) C1–C2	BD*(2) C3–C4	9.72	0.30	0.069
BD (2) C1–C2	BD*(2) C5–C6	10.17	0.27	0.068
BD (2) C3–C4	BD*(2) C1–C2	8.43	0.27	0.062
BD (2) C3–C4	BD*(2) C5–C6	9.94	0.26	0.067
BD (2) C3–C4	BD*(2) C10–O11	6.70	0.32	0.059
BD (2) C5–C6	BD*(2) C1–C2	12.34	0.27	0.074
BD (2) C5–C6	BD*(2) C3–C4	8.68	0.30	0.065
LP (1) O11	RY*(1) C10	7.73	1.88	0.152
LP (2) O11	BD*(1) C3–C10	10.55	0.63	0.105
LP (2) O11	BD*(1) C10–O12	15.59	0.64	0.128
LP (2) O12	BD*(2) C10–O11	24.83	0.34	0.117
LP (2) O14	BD*(2) C1–C2	14.48	0.34	0.096
LP (1) N16	BD*(2) C5–C6	18.06	0.30	0.101
BD*(2) C1–C2	BD*(2) C3–C4	55.17	0.03	0.078
BD*(2) C3–C4	BD*(2) C10–O11	42.00	0.02	0.071
BD*(2) C5–C6	BD*(2) C3–C4	54.44	0.03	0.079

E' means energy of hyperconjugative interactions [$E^{(2)}$]

$\Delta E = E_j - E_i$ is the energy difference between donor (i) and acceptor (j) NBO orbitals; $F = F(i, j)$ is the Fock matrix element between i and j NBO orbitals

A typical mass spectrum of MZ is shown in Figs. 2 and 3 at 70 and 15 eV, respectively.

At 15 eV only molecular ion and fragment ion at $m/z = 135$ which can be assigned to $[C_7H_5NO_2]^+$due to H_2O loss from the molecular ion, i.e., $[M–H_2O]^+$. On the other hand, spectrum of MZ at 70 eV is characterized by competitive and consecutive pathways (Scheme 1). Prominent fragment ions at 70 eV lies between fragment ion at $m/z = 52$ up to molecular ion $[C_7H_7NO_3]^+$ at $m/z = 153$. However, the fragment ion, $[C_7H_5NO_2]^+$, represents the most prominent fragment ion at 70 eV (base peak RI = 100 %) and 12–6 % at 15 eV (Figs. 2, 3). The highest relative intensity of this fragment ion ($[C_7H_5NO_2]^+$, $m/z = 135$) may be due to the presence of electrons lone pair of oxygen and nitrogen atom, which stabilizes the fragment by delocalization. The second prominent ion is the one observed at $m/z = 79$, this fragment ion is mildly due to successive loss of H_2O to CO (acetyl) to CO from ring. Molecular ion, $[C_7H_7NO_3]^+$, observed at $m/z = 153$ represents the third prominent ion in the mass spectrum and it has a relatively high stability (RI = 58.1 %). Based on the data obtained from MS at 70 and 15 eV, one can rationalize the proposal principle pathway of MS molecule at 70 eV as shown in Scheme 1.

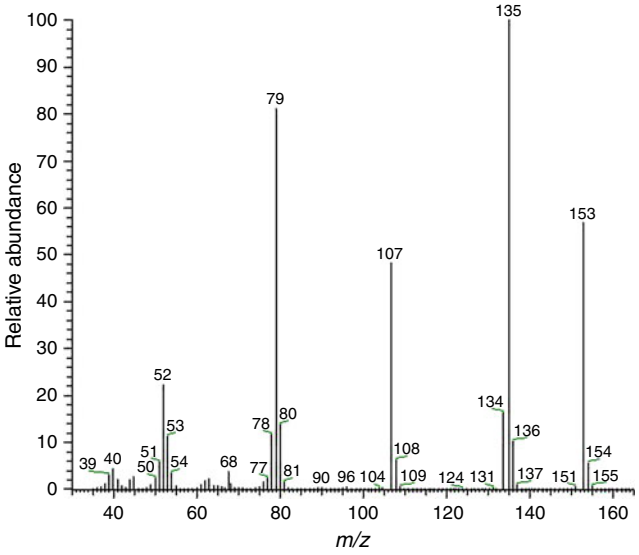

Fig. 2 Mass spectrum of mesalazine at 70 eV

Thermal analysis

Thermal analyses of the drugs are an important tool to get information about the thermal stability. The thermogravimetric analysis (TG and DTG) curves of MZ (Fig. 4) were displayed within temperature range 25–700 °C.

The TG curve of MZ drug (Fig. 4) refers to two stages of mass loss at temperature range from 225 to 650 °C. The first estimated mass loss of 75.3 % (calcd. 75.0 %) within the temperature range 225–350 °C, and a second stage, within the temperature range 350–650 °C, assigned for decomposition of the remaining part, $[C_3H_2]$, with an estimated mass loss of 25.3 % (calcd. 24.8 %). From the first mass loss (75.3 %) observed in TG curve, one can propose that the mass loss may be due to successive decomposition steps, with fast rate, which consequently are merged together and appeared as one step on the TG curve, as shown in Scheme 2. Then the produced C_3H_2 species is slowly decomposed in temperature range 350–650 °C in a two overlapped steps with an estimated mass loss of 25.3 %. Moreover, these results are confirmed by deep inspection of the DTG curve (Fig. 4), since it showed an asymmetric peak at about 300 °C. This asymmetric peak indicates that this peak is due to two or more merged decomposition steps. Additionally, the second step (mass loss of 25.3 % in the temperature range 350–650 °C) in the TG curve could be solved into two broad and small peaks on the DTG curve which consequently might give an indication that the last proposed intermediate in the thermal decomposition steps (Scheme 2) might decompose in two or more steps.

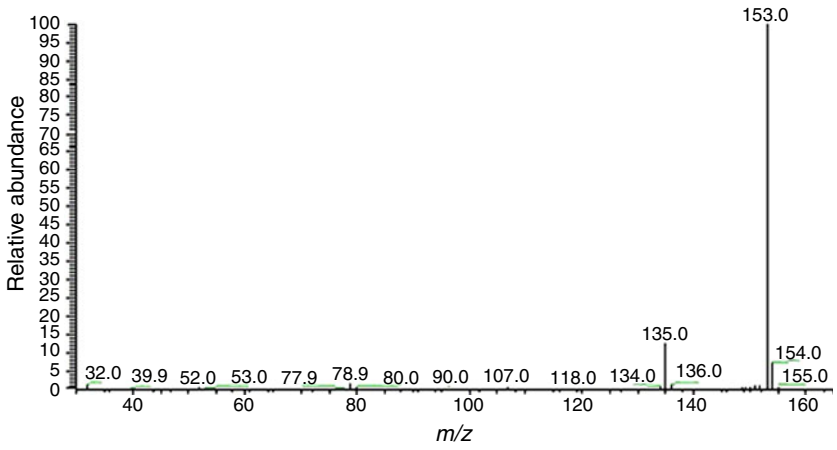

Fig. 3 Mass spectrum of mesalazine at 15 eV

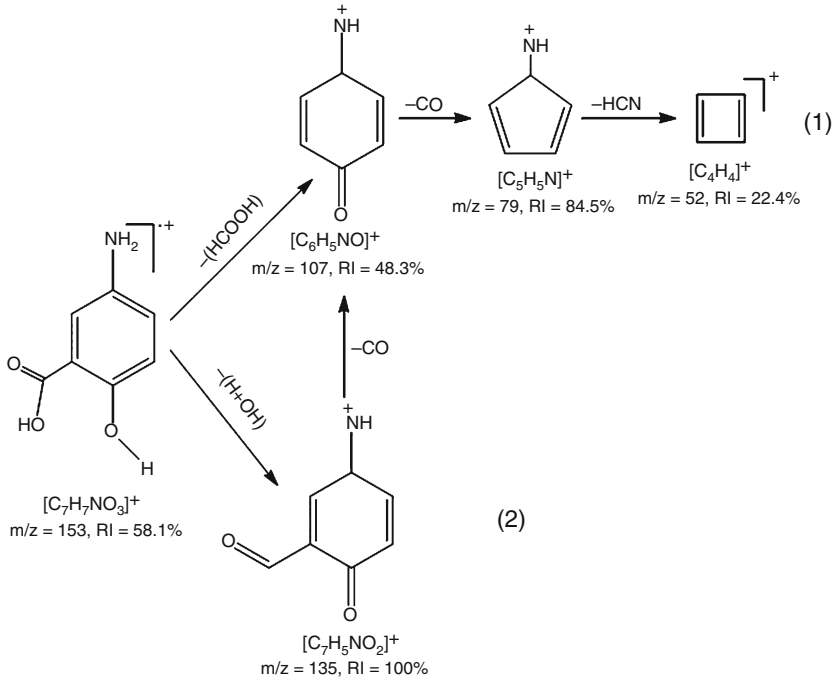

Scheme 1 Fragmentation pathway of principal fragmentation of mesalazine at 70 eV

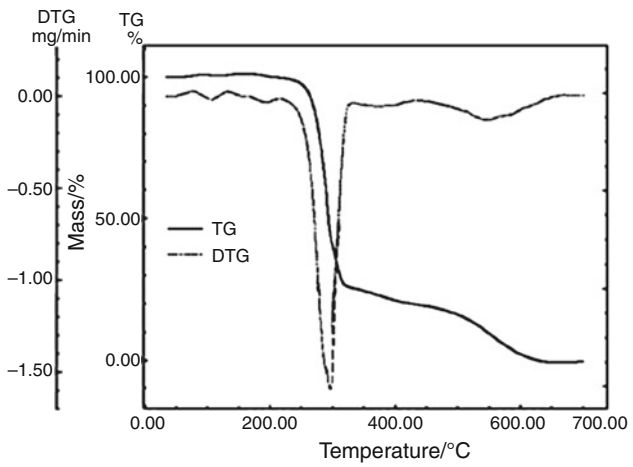

Fig. 4 Thermal analyses TG and DTG of mesalazine drug

Correlation between mass spectral fragmentation, DFT calculations, and NBO analysis of the charged MZ molecule

The scope of this investigation is restricted to a search for prediction of the initial bond ruptures during the course of fragmentation of MZ molecule. Empirical observation indicates that the course of subsequent fragmentation is determined to large extent by the initial bond rupture of molecular ion in MS [35]. Mass spectral fragmentation of MZ revealed two important competitive pathways (Scheme 1, processes 1 and 2). MZ fragmented by loss of HCOOH (formic acid) (process 1) forming a fragment ion at $m/z = 107$ $[C_6H_5NO]^+$ (RI = 48.3 %), and/or by successive loss of H_2O (ortho effect) followed by CO (process 2) forming a fragment ion at $m/z = 135$ $[C_7H_5NO_2]^+$

Scheme 2 Proposed thermal decomposition of mesalazine

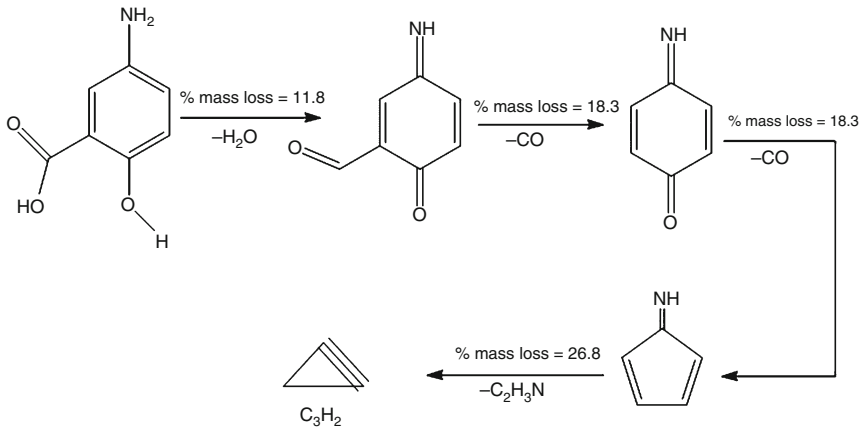

(RI = 100 %) and at $m/z = 107$. DFT calculations and NBO analysis revealed that the C3–C10 bond has the lowest bond order (0.9717) of charged system and large bond length (1.515 Å) (Table 1). Consequently, one can expect the loss of HCOOH is the first rupture. On the other hand, C10–O12 bond is the second weakest bond (bond order = 1.092 and bond length = 1.3328 Å) (Table 1), resulting a rupture of H_2O (OH acetyl and H from OH ring due to proximity effect). Interestingly, it can be concluded that C10–O12 bond is the first bond rupture for charged system for the following reasons:

i. Small difference in bond order between processes 1 and 2 ($\approx$0.120).
ii. Presence of only prominent of $[M–H_2O]^+$ at low energy (15 eV), Fig. 3, with RI = 12.6 % indicating that $[M\text{-}H_2O]^+$ is the first appearance in fragmentation of MZ.
iii. According to the NBO analysis, the electrostatic attraction between C_3 (−0.15109) and C_{10} (0.78726) process 1 is larger than that between C_{10} (0.78726) and O_{12} (−0.64678) process 2, as presented in Table 2.
iv. Electron density of the anti-bonding orbital BD*(1) C10–O12 is larger than that of BD*(1) C3–C10, as concluded from NBO analysis, Table 4.

Subsequent loss of CO and HCN from $[C_6H_5NO]^+$ gives fragments $[C_5H_5NO]^+$ and $[C_4H_4]^+$ ions, respectively; (Scheme 1, process 1). It is known that the organic molecule is more stable in neutral state than in ionic one [23].

Correlation of the TA behavior, DFT calculations, and NBO analysis of the neutral MZ molecule

As indicated previously, using of quantum calculations to determine the initial bond cleavage, in a predicative manner, would be an importantly first step. On the basis of the computational data for the neutral MZ molecule, although C3–C10 bond has lower bond order (1.0250) and larger bond length (1.4899 Å) compared to C10–O12 bond, which has bond order of 1.0552 and bond length of 1.3497 Å, it is expected that C10–O12 bond is the first site of cleavage followed by C3–C10 bond rupture. This conclusion is reached for the following reasons: Small difference in bond order is present between C3–C10 and C10–O12 bonds ($\approx$0.030); according to the NBO analysis, the electrostatic attraction forces between C3 (−0.19836) and C10 (0.79193) are larger than that between C10 (0.79193) and O12 (−0.66297); and according to the NBO analysis, interaction of the lone pair LP(2) O11 with the antibonding orbital of C10–O12 bond is higher than that its interaction with the antibonding orbital of C3–C10 bond which means in turn that BD*(1) C10–O12 has higher electron density compared with that of BD*(1) C3–C10. Consequently, as mentioned previously, it is expected that the neutral MZ molecule undergoes cleavage of C10–O12 bond first to loss H_2O (OH from rupture of C10–O12 bond and H from the phenolic OH group) followed by rupture of C3–C10 bond giving off CO. After that, according to the quantum data presented in Tables 1, 2, and 3, it can be concluded that the C2–O14 bond will then be decomposed followed by C5–N16 bond cleavage because the former has smaller bond order and electrostatic interaction than the latter. The explanations obtained by DFT calculations and NBO analysis agreed well with the TA degradation because the neautral MZ molecule decomposed to give off H_2O, CO, CO, and then C_2H_3N in temperature range 200–350 °C leaving the more stable part C_3H_2 which decomposed in the temperature range 350–650 °C.

Correlation between TA and MS

It is important to make a comparison between the results of TA and MS of MZ drug, to see the behavior of the drug in both techniques. This comparison shows the agreement and disagreement on the fragmentation pathways. In MS the

main fragmentation pathway (Scheme 1, process 1) is successive loss of H_2O to CO to CO forming a fragment ion $[C_5H_5N]^+$ which decomposes by loss of HCN forming a fragment ion $[C_4H_4]^+$ ($m/z = 52$, RI = 22.4 %). In TA the decomposition mechanism is compatible with that obtained from MS except that the formed neutral C_5H_5N can be decomposed in TA to give C_2H_3N and C_3H_2 molecules. Additionally, C_2H_3N is thermally decomposed in the first temperature range 225–350 °C, and the remainder C_3H_2 is decomposed in the temperature range 350–650 °C.

Conclusions

This study provides an application of experimental MS and TA techniques and theoretical investigation using DFT calculations and NBO analysis on MZ drug. From the application of both practical and theoretical, it is concluded that: The primary fragmentation of MZ, is the loss of H_2O molecule. Subsequent fragmentation in MS is by loss of successive loss of CO (ring) forming finally C_4H_4 fragment at $m/z = 52$. In TA, MZ is dissociated completely in the temperature range 225–650 °C, while the molecular ion can be fragmented after few electron volts above the ionization energy (8.64 eV). Theoretical DFT calculations and NBO analysis could help to choose the most probable fragmentation pathway in both MS and TA techniques.

References

1. Sands BE. Therapy of inflammatory bowel disease. Gastroenterology. 2000;118:68S–82S.
2. Mura P, Faucci MT, Maestrelli F, Furlanetto S, Pinzauti S. Characterization of physicochemical properties of naproxen systems with amorphous β-cyclodextrin–epichlorohydrin polymers. J Pharmaceut Biomed. 2000;29:1015–24.
3. Sandborn WJ, Feagan BG, Lichtenstein GR. Medical management of mild to moderate Crohn's disease: evidence-based treatment algorithms for induction and maintenance of remission. Aliment Pharm Therap. 2007;26:987–1003.
4. Larsen BS, McEwen CN, editors. Mass spectrometry of biological materials. New York: Marcel Dekker; 1998.
5. Levsen K. Fundamental aspects of organic mass spectrometry. Weinheim/New York: Verlag Chemie; 1978.
6. Bourcier S, Hoppiliard Y. Fragmentation mechanisms of protonated benzylamines. Electrospray ionisation-tandem mass spectrometry study and ab initio molecular orbital calculations. Eur J Mass Spectrom. 2003;9:351–60.
7. Das KG, James EP. Organic mass spectrometry. New Delhi: Oxford and IB11 Publishing Co.; 1976.
8. Soliman MH, Mohamed GG. Cr(III), Mn(II), Fe(III), Co(II), Ni(II), Cu(II) and Zn(II) new complexes of 5-aminosalicylic acid: spectroscopic, thermal characterization and biological activity studies. Spectrochim Acta, Part A. 2013;107:8–15.
9. Barbas R, Prohens R, Puigjaner C. A new polymorph of Norfloxacin. J Therm Anal Calorim. 2007;89:687–92.
10. Pentak D, Sułkowski WW, Sułkowska A. Calorimetric and EPR studies of the thermotropic phase behavior of phospholipid membranes. J Therm Anal Calorim. 2008;93:471–7.
11. Picker-Freyer KM. An insight into the process of tablet formation of microcrystalline cellulose. J Therm Anal Calorim. 2007;89:745.
12. Santos AFO, Basílio ID Jr, de Souza FS, Medeiros AFD, Pinto MF, de Santana DP, Macêdo RO. Application of thermal analysis in study of binary mixtures with metformin. J Therm Anal Calorim. 2008;93:361–4.
13. Michalik K, Drzazga Z, Michnik A. Calorimetric characterization of 2′,3′-dideoxyinosine water solution. J Therm Anal Calorim. 2008;93:521–6.
14. Błażejowski J, Zadykowicz B. Computational prediction of the pattern of thermal gravimetry data for the thermal decomposition of calcium oxalate monohydrate. J Therm Anal Calorim. 2013;113:1497–503.
15. Su H, Liu Z. The structure and thermal properties of novel DOPO-containing 1,3-benzoxazines. J Therm Anal Calorim. 2013;114:1207–15.
16. Koleżyński A, Małecki A. Theoretical studies of electronic structure and structural properties of anhydrous alkali metal oxalates. J Therm Anal Calorim. 2013;114:1391–9.
17. Fahmey MA, Zayed MA, Keshk YH. Comparative study on the fragmentation of some simple phenolic compounds using mass spectrometry and thermal analyses. Thermochim Acta. 2001;366:183–8.
18. Fahmey MA, Zayed MA. Phenolic-iodine redox products: mass spectrometry, thermal and other physico-chemical methods of analyses. J Therm Anal Calorim. 2002;67:163–75.
19. Fahmey MA, Zayed MA, El-Shobaky HG. Study of some phenolic-iodine redox polymeric products by thermal analyses and mass spectrometry. J Therm Anal Calorim. 2005;82:137–42.
20. Somogyi A, Gömöry A, Vékey K, Tamás J. Use of bond orders and valences for the description and prediction of primary fragmentation processes. Org Mass Spectrom. 1991;26:936–8.
21. Zayed MA, Fahmey MA, Hawash MF. Investigation of malomananilide and its dinitro-isomers using thermal analyses, mass spectrometry and semi-empirical MO calculations. Egypt J Chem. 2005;48(1):43–57.
22. Zayed MA, Fahmey MA, Hawash MF. Investigation of diazepam drug using thermal analyses, mass spectrometry and semi-empirical MO calculation. Spectrochim Acta, Part A. 2005;61:799–805.
23. Zayed MA, Hawash MF, Fahmey MA. Structure investigation of codeine drug using mass spectrometry, thermal analyses and semi-emperical molecular orbital (MO) calculations. Spectrochim Acta, Part A. 2006;64:363–71.
24. Zayed MA, Fahmey MA, Hawash MF, El-Habeeb AA. Mass spectrometric investigation of buspirone drug in comparison with thermal analyses and MO-calculations. Spectrochim Acta, Part A. 2007;67:522–30.
25. Frisch MJ, Trucks GW, Schlegel HB, Scuseria GE, Robb MA, Cheeseman JR, Scalmani G, Barone V, Mennucci B, Petersson GA, Nakatsuji H, Caricato M, Li X, Hratchian HP, Izmaylov AF, Bloino J, Zheng G, Sonnenberg JL, Hada M, Ehara M, Toyota K, Fukuda R, Hasegawa J, Ishida M, Nakajima T, Honda Y, Kitao O, Nakai H, Vreven T, Montgomery JA Jr, Peralta JE, Ogliaro F, Bearpark M, Heyd JJ, Brothers E, Kudin KN, Staroverov VN, Keith T, Kobayashi R, Normand J, Raghavachari K, Rendell A, Burant JC, Iyengar SS, Tomasi J, Cossi M, Rega N, Millam JM, Klene M, Knox JE, Cross JB, Bakken V, Adamo C, Jaramillo J, Gomperts R, Stratmann RE, Yazyev O, Austin AJ, Cammi R, Pomelli C, Ochterski JW, Martin RL, Morokuma K, Zakrzewski VG, Voth GA, Salvador P, Dannenberg JJ, Dapprich S, Daniels AD, Farkas O, Foresman JB, Ortiz JV, Cioslowski J, Fox DJ. Gaussian 09. Revision C01. Wallingford: Gaussian Inc.; 2010.

26. Becke AD. Density functional thermochemistry. III. The role of exact exchange. J Chem Phys. 1993;98:5648–52.
27. Lee C, Yang W, Parr RG. Development of the Colle–Salvetti correlation-energy formula into a functional of the electron density. Phys Rev B. 1988;37:785–9.
28. Glendening ED, Badenhoop JK, Reed AE, Carpenter JE, Weinhold F. NBO. Version 3.1. Madison: Theoretical Chemistry Institute, University of Wisconsin; 1995.
29. Li XH, Zhang RZ, Zhang XZ. Natural bond orbital analysis of some para-substituted *N*-nitrosoacetanilide biological molecules. Struct Chem. 2009;20:1049–54.
30. Chocholousova J, Spirko V, Hobza P. First local minimum of the formic acid dimer exhibits simultaneously red-shifted O–H···O and improper blue-shifted C–H···O hydrogen bonds. Phys Chem Chem Phys. 2004;6:37–41.
31. Reed AE, Curtiss LA, Weinhold F. Intermolecular interactions from a natural bond orbital, donor–acceptor viewpoint. Chem Rev. 1988;88:899–926.
32. Computer program GaussView Version 5.0.9, Gaussian, Wallingford.
33. Hrušák J, Tkaczyk M. Mn do study of fragmentations in mass spectrometry. Part II. Substituent effects in the ioinization of [CH_3–CO–R] compounds and their enol tautomers. Org Mass Spectrom. 1990;25:214–8.
34. Choo J, Kim S, Joo H, Kwon Y. Molecular structures of (trifluoromethyl)iodine dihalides CF_3IX_2 (X = F, Cl): ab initio and DFT calculations. J Mol Struct (Theochem). 2002;587:1–8.
35. Loew G, Chadwick M, Smith D. Applications of molecular orbital theory to the interpretation of mass spectra. Prediction of primary fragmentation sites in organic molecules. Org Mass Spectrom. 1973;7:1241–51.